Neoclassical impurity transport in full-f global GYSELA simulations

D. Estève, X. Garbet, Y. Sarazin, S. Breton, Ph. Ghendrih, V. Grandgirard, T. Cartier-Michaud, G. Dif-Pradalier, C. Norscini
CEA, IRFM, F-13108 St.Paul-lez-Durance cedex, France

Introduction

The computation of impurity transport in magnetized plasmas has gained a renewed interest for several reasons. Firstly an increasing number of tokamaks operate with tungsten plasma facing components in order to prepare the operation of Iter [1, 2]. Recent results from ASDEX-Upgrade [3] and JET [4] indicate that tungsten transport plays an essential role in the discharge history. Accumulation in the core may lead to reduced performances, and in some cases to radiative collapses. Secondly impurity seeding of edge plasmas with medium charge numbers Z such as argon or neon is envisaged in Iter [5]. Inward penetration of these impurities should be prevented to avoid core dilution and a subsequent decrease of the fuel concentration. Finally fusion reactions will produce helium, which must be extracted efficiently, again to avoid core dilution. Neoclassical impurity transport has been investigated in details in the 80' [6, 7], and updated recently to account for poloidal asymetries due to centrifugal forces and/or RF heating [8, 9, 10]. Impurity fluxes are traditionally written as sums of turbulent and neoclassical contributions. However synergistic effects cannot be excluded so that it is desirable to compute these two contributions on an equal footing, at least to verify this hypothesis. The right framework for computing neoclassical and turbulent transport at the same time appears to be a set of gyrokinetic equations that account for collisions. This paper presents the first results of the GYSELA code with a new collision operator that has been implemented recently for this purpose.

Model collision operator implemented in the GYSELA code

The collision operator that is implemented in the GYSELA code is of the form $C_a = \sum_b C_{ab}$ with

$$\begin{aligned} C_{ab}(\bar{F}_a) &= \frac{\partial}{\partial v_\parallel}\left[D_{d,ab}F_{M0a}\frac{\partial}{\partial v_\parallel}\left(\bar{f}_a - \frac{m_a v_\parallel U_{\parallel d,a}}{T_a}\right)\right] \\ &- \nu_{s,ab}\frac{m_a v_\parallel}{T_a}\left(U_{\parallel d,a} - U_{\parallel ba}\right)F_{M0a} \\ &+ \frac{2}{3}\frac{1}{N_a T_a}\left(Q_{ab} + V_{\parallel a}R_{\parallel ab} + q_{ab}\right)\left(\frac{m_a v^2}{2T_a} - \frac{3}{2}\right)F_{M0a} \end{aligned} \quad (1)$$

where $\bar{f}_a$ is the gyrocenter distribution $\bar{F}_a$ normalized to the Maxwellian F_{M0a}, $D_{d,ab}$ is the deflection diffusion coefficient and $\nu_{s,ab}$ is the slowing-down collision rate, Q_{ab} is the energy collisional transfer rate, $R_{\parallel ab}$ is the friction force, N_a the density, m_a the mass, and T_a the temperature. The function $U_{\parallel d,a}(v)$ and parameters $U_{\parallel ab}$ and q_{ab} are adjusted to conserve momentum and energy, i.e.

$$\frac{m_a v}{T_a}U_{\parallel d,a}(v) = \frac{3}{4\pi}\int 2\pi d\xi\,\xi\,\bar{f}_a \quad (2)$$

$$U_{\parallel ab} = \frac{\left\langle \nu_{s,ab}v^2 U_{\parallel d,a}\right\rangle_a}{\left\langle \nu_{s,ab}v^2\right\rangle_a} \quad (3)$$

$$q_{ab} = N_a T_a \left\langle \sigma_{ab} \bar{f}_a \right\rangle_a \tag{4}$$

and $\xi = v_\parallel / v$ is the pitch-angle parameter and v the velocity modulus. The bracket indicate an average over F_{M0a}, and the function $\sigma_{ab}(v)$ is given by

$$\sigma_{ab}(v) = -\nu_{d,ab} \frac{m_a v^2}{2T_a} v_\parallel \frac{\partial}{\partial v_\parallel} \ln \left(D_{d,ab} F_{M0a} v_\parallel \right) \tag{5}$$

This multi-species collision operator satisfies several constraints: particle, momentum and energy conservation, and it relaxes towards a Maxwellian in the direction parallel to the magnetic field.

Numerical tests of the collision operator

The operator Eq.(1) has been implemented in the GYSELA code. Its main properties have been verified, as detailed and illustrated in the following. The gyrokinetic equation is reduced to its collisional part only, i.e. the Lagrangian derivative along the particle trajectories is ignored. Keeping only one species allows a test of the conservation properties of the like-particle collision operator. In a second stage, a trace impurity is added and the transfer rates of momentum and energy from one species to another are computed. The main ion species is deuterium while impurities are helium, carbon and tungsten, in the trace limit $N_Z Z^2 \ll N_D$. A typical grid is (N_r, N_θ, N_φ, $N_{v_\parallel}$,N_μ) = (64,64,8,256,32).

Particle, momentum and energy conservation laws have been checked by running the code in the single particle case, with an initial distribution function that is a centered Maxwellian. The density, parallel velocity and temperature radial profiles are constant, and their normalized values are initialized to one. For each fluid quantity X_D, the absolute error $\delta X_D = |X_D(t) - X_D(t=0)|$ is calculated at mid-radius after a deuterium collision time $t = \tau_{DD}$. The normalized collisionality is $\nu_D^\star = (a/R_0)^{-3/2} \nu_D (qR_0/v_{TD}) = 2$. The errors are found to be $\delta N_D \simeq 10^{-9}$, $\delta V_{\parallel D} \simeq 10^{-12}$ and $\delta T_D \simeq 10^{-5}$. These errors are negligible when compared to the typical increments of the fluid quantities due to transport and sources during the same time lags.

Relaxation towards a Maxwellian is tested by initializing the code with a distribution function that is far from a Maxwellian in the parallel direction. Figure 1 shows that the initial state (fig. 1a) relaxes towards a Maxwellian distribution function (fig. 1b). The exchange of momen-

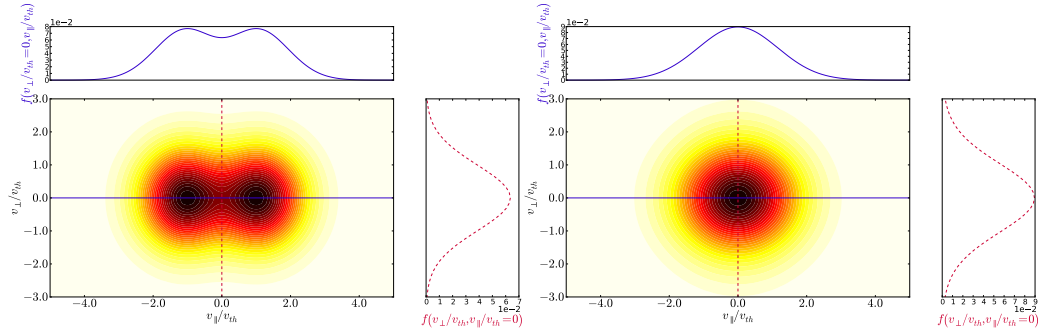

(a) (b)

Figure 1: 2D plot in the velocity space of the distribution function at initial (a) and final (b) time.

tum between the impurity and the main ions is investigated first. The code is initialized with a

deuterium distribution function that is a shifted Maxwellian in the low Mach number limit, with $V_{\|i}/v_{Ti} = 0.05$. The initial distribution function of the impurity is a centered Maxwellian. Density and temperature profiles are flat with $T_D = T_Z$. The evolution of the mean parallel velocity is given by

$$\partial_t V_{\|a} = -\nu_{ab}(V_{\|a} - V_{\|b}) \tag{6}$$

where ν_{ab} is the momentum collisional transfer rate. In the case of thermal relaxation, the initial distribution function is a centered Maxwellian with constant density. The initial deuterium temperature is chosen larger than the impurity temperature, $T_D > T_Z$. The time evolution of each temperature is dictated by an equation similar to Eq.(6), with velocities replaced by temperatures. The time evolution of the mean velocity and temperature differences are shown on figure 2. The collisional damping rates are found to agree with the theoretical values.

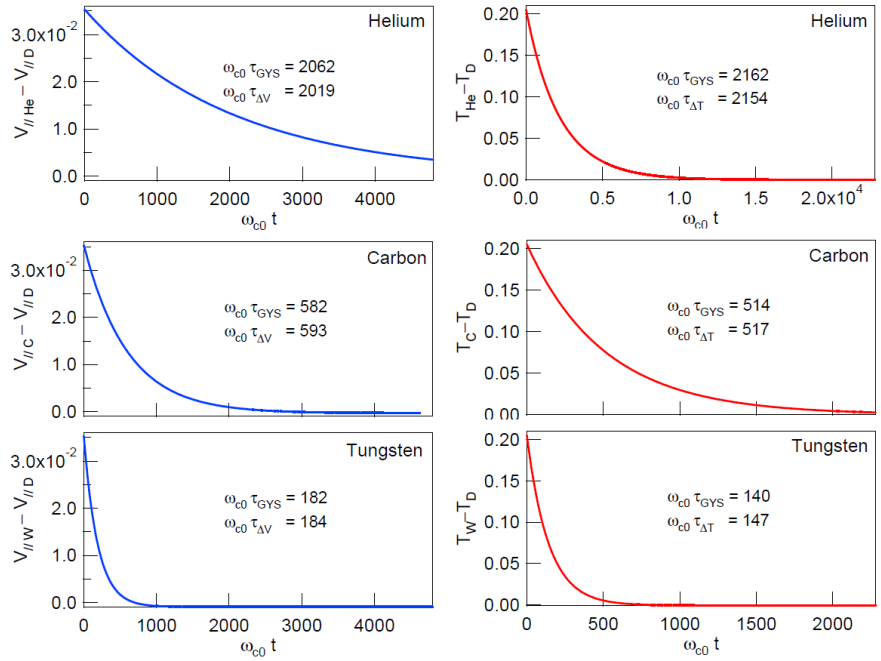

Figure 2: Time evolution of the difference between the parallel flow and temperature of the main ion species and those of helium, carbon and tungsten impurities.

Recovering the theory of impurity neoclassical transport

A more challenging test consists in recovering the neoclassical theory of impurity transport. In this case, the Lagrangian derivatives along the particle trajectories are retained. We consider here the case where the main ion species is deuterium in banana regime, while the second species is a trace impurity in various collision regimes, depending on mass and charge. Gradients are below the instability threshold (no turbulence), so that collisional transport only is left. The expression of the impurity flux is known to be of the form

$$\Gamma_Z = -D_Z N_Z \left(\frac{\partial \ln N_Z}{\partial r} - Z\frac{\partial \ln N_i}{\partial r} - HZ\frac{\partial \ln T}{\partial r} \right) = -D_Z \frac{\partial N_Z}{\partial r} + V_Z N_Z$$

where D_Z is diffusion coefficient, V_Z the pinch velocity and r the minor radius. The thermal screening factor H is known to be equal to $-1/2$ in the Pfirsch-Schlüter regime. In a first step,

all gradients are set to zero except the impurity density gradient. In that case diffusion only is expected. The diffusion coefficient is determined by plotting the impurity flux $\frac{\Gamma_Z}{N_Z}$ versus the density gradient $-\frac{\partial N_Z}{N_Z \partial r}$ for several values of the gradient. Points lay on a line and the slope is the diffusion coefficient D_Z. The diffusion coefficient agrees well with the analytical calculation and values given by the neoclassical code NEO [11], as shown in Fig.3a. A second test consists in setting a finite main ion density gradient. In that case, an impurity accumulation is expected. The ratio $\frac{V_Z}{D_Z}$ is found by plotting again the flux versus the gradient. It is equal to the value of $\frac{\partial N_Z}{N_Z \partial r}$ such that the flux vanishes. It is found to agree with the theoretical expectation $Z\frac{\partial N_i}{N_i \partial r}$, as shown in Fig.3b.

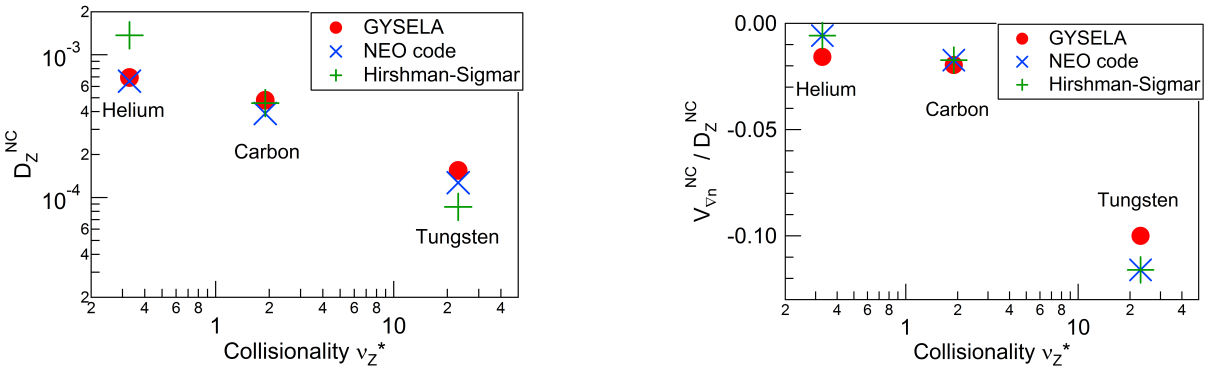

Figure 3: (a) Diffusion coefficient of helium, carbon and tungsten compared with the Hirshman-Sigmar analytical prediction and values calculated with the NEO code. (b) Same legend for the ratio V_Z/D_Z.

Conclusion

A linearized multi-species collision operator has been implemented in the GYSELA gyrokinetic code. This operator has been numerically tested and is found to satisfy particle, momentum and energy conservation with an excellent accuracy. Also it relaxes towards a Maxwellian. Moreover the interspecies relaxation rates for momentum and energy well agree with the theoretical values. The code is also found to recover the main results of theory for impurity neoclassical transport. The diffusion coefficients are found to agree with analytical expressions and also with the NEO code. In the isothermal limit, accumulation is found due to the main ion density gradient. Thermal screening effect is being currently tested and first results are encouraging.

References

[1] R. Neu, M. Balden, V. Bobkov, *et al.*, Plasma Phys. Control. Fusion **49**, B59 (2007).
[2] R. Neu, G. Arnoux, M. Beurskens, et al., Phys. Plasmas **20**, 056111 (2013).
[3] M. Sertoli, C. Angioni, R. Dux et al.,Plasma Phys. Control. Fusion **53**, 035024 (2011).
[4] C. Angioni, P. Mantica, T. Pütterich, *et al.*, Nucl. Fusion **54**, 083028 (2014).
[5] A. Loarte, B. Lipschultz, A.S. Kukushkin et al., Nucl. Fusion **47** S203 (2007).
[6] S.P. Hirshman and D.J. Sigmar, Physics of Fluids **20**, 418 (1977).
[7] S.P. Hirshman and D.J. Sigmar, Nucl. Fusion **21**, 1079 (1981).
[8] M. Romanelli and M. Ottaviani, Plasma Phys. Control. Fusion **40**, 1767 (1998).
[9] C. Angioni and P. Helander, Plasma Phys. Control. Fusion **56**, 124001 (2014).
[10] E. A. Belli, J. Candy and C. Angioni, Plasma Phys. Control. Fusion **56**, 124002 (2014).
[11] E. A. Belli and J. Candy Plasma Phys. Control. Fusion **50**, 095010 (2008).